Application of an optimal estimation inverse method to GPS/MET bending angle observations

JOURNAL OF GEOPHYSICAL RESEARCH, VOL. 106, NO. D15, PAGES 17,147–17,160, AUGUST 16, 2001

Application of an optimal estimation inverse method to GPS/MET bending angle observations

Paul I. Palmer[1] and John J. Barnett

Department of Physics, Clarendon Laboratory, Oxford, England

Abstract. *Palmer et al.* [2000] describes an optimal estimation inverse method for radio occultation (RO) bending angle measurements to retrieve simultaneously temperature, humidity, and surface pressure; outlines quality control procedures for retrieved profiles; and investigates the results from numerical simulations. Here we present retrievals that use bending angle observations from the Global Positioning System Meteorology (GPS/MET) satellite instrument and a priori information from the European Centre for Medium-Range Weather Forecasts analyses. Retrieved profiles are compared with correlative radiosondes, United Kingdom Meterological Office (UKMO) model analyses, and retrievals from the conventional inverse method. Retrieved temperature profiles are generally colder than analyses but agree with the conventional inverse method to within 1 K. Water vapor retrievals are generally drier than the UKMO analyses and wetter than the radiosonde profiles. Quality of retrieved surface pressure values are related to the extent to which RO observations reach into the troposphere. Low-latitude retrievals make large adjustments to surface pressure and tropospheric temperatures, which are directly linked to the lack of water vapor above 300 hPa in the inverse model, consistent with previous studies. A study of individual occultations at low and high latitude shows that the optimal retrievals are able to resolve small-scale atmospheric structure exhibited by the conventional inverse method and collocated radiosondes, not shown by analyses.

1. Introduction

The Global Positioning System/Meteorology (GPS/MET) experiment is a modified GPS receiver aboard the MicroLab-1 satellite (launched in April 1995). The GPS/MET instrument uses the radio occultation (RO) technique to obtain meteorological data. Transmitted signals from the GPS satellites passing through Earth's atmosphere are delayed due to refraction effects. This phase delay can be inverted to obtain vertical profile information about the neutral atmosphere. The cumulative effect of the atmosphere on the ray path taken by the GPS-transmitted signal can be expressed in terms of the total refractive bending angle as a function of the impact parameter. The impact parameter may be defined as the perpendicular distance between the local center of curvature of the Earth at the tangent point of the ray and the asymptotic straight line followed by the ray as it approaches the atmosphere. *Kursinski et al.* [1997] give a detailed description of the method used to measure the RO atmospheric observables for the Earth.

Initial GPS/MET data showed that the retrieved profiles compared well with collocated radiosondes and numerical weather prediction (NWP) analyses [*Kursinski et al.*, 1996; *Ware et al.*, 1996]. Further validation of these data have been undertaken by *Rocken et al.* [1997]. *Rocken et al.* [1997] used a variety of correlative data and found that GPS/MET data agreed within 1 K with the best correlative data sets between 1 and 40 km. The GPS RO data have an all-weather capability (i.e., it is not affected significantly by clouds or aerosols) and is also self-calibrating. Unlike most other remote sensing techniques, which measure the amplitude of a signal, GPS RO measures a time delay for which measurement techniques are potentially much more accurate (and already need to be in place for correct GPS operation). Vertical resolution of RO measurements of Earth's atmosphere, which varies from 0.5 km near surface to 2 km in the upper troposphere and stratosphere [*Kursinski et al.*, 1997], is limited by diffraction. Radio occultation observations of Earth's atmosphere using the GPS therefore represent an important data type for NWP and a potential tool to monitor climate variability.

The radio occultation observation is primarily affected by temperature and water vapor along the ray path taken through the neutral atmosphere. There is no information inherent in this observation which allows the separation of temperature and humidity. The conventional method of inverting bending angle measurements to obtain temperature and humidity involves the use of an integral transform to obtain a profile of refractivity as a function of geometric height [*Fjeldbo and Eshleman*, 1968]. The hydrostatic re-

[1] Now at Division of Engineering and Applied Sciences, and Department of Earth and Planetary Sciences, Harvard University, Cambridge, Massachusetts

Paper number 2001JD900205.
0148-0227/01/2001JD900205$09.00

lation is then used to obtain pressure and temperature from refractivity via density. In the presence of small amounts of water vapor a correction can be made in this retrieval step, involving an interative procedure assuming a priori water vapor information. If the water vapor contribution to the bending angle observation becomes too large (e.g., in the tropics), this "low water vapor correction" is inadequate, and the partial water vapor pressure should be retrieved, assuming a priori temperature information. This represents a suboptimal method of retrieving temperature and humidity since there is no guarantee of consistency between the retrieved temperature and the humidity values. We denote this method of inverting bending angle observations the analytic inverse method since it is largely based on an analytic integral transform. Inadequate modeling of refractivity inhomogeneities along the transmitter–receiver path (hereinafter referred to as horizontal gradients) can cause large retrieval errors when using the analytic inverse method [*Ahmad and Tyler*, 1999]. For Earth's atmosphere, where a reasonable prior knowledge of horizontal gradients is available, the analytic inversion does not represent the most suitable inverse method for radio occultation observations. The suboptimal way the analytic method retrieves temperature and water vapor simultaneously using prior values, together with the inability of the analytic method to account for horizontal refractivity inhomogenieties, represents two key disadvantages to the analytic inverse method.

Eyre [1994] addresses these issues and suggests a statistically optimal retrieval approach, using variational methods, to enable the direct assimilation of bending angle [*Palmer et al.*, 2000], refractivity [*Healy and Eyre*, 2000], or retrieved profiles of temperature and humidity into a NWP model. The bending angle observations have the advantage of being in a "raw" form, so modeling their error characteristics is relatively straighforward since they can be considered independent and therefore uncorrelated with each other. In the strictest sense, the measured phase delay signal is the "raw" observation. Bending angle measurements are found to have a small, local correlation between successive levels due to filtering of the phase measurements [*Luntama*, 1997], but to a good approximation can be considered uncorrelated. Refractivity measurements have the advantage of a simpler forward model which can be readily differentiated to allow the tangent linear operator to be expressed analytically, thus allowing a more expedient retrieval. However, refractivity error estimates are more difficult to model since the errors on bending angle measurements become highly correlated due to the application of the integral transform. Temperature measurements offer an even simpler forward model, but the suboptimal method of retrieving temperature and water vapor using the analytic inverse method leads to errors that are difficult to model correctly. The choice of the variable to assimilate directly then becomes a trade-off between the complexity of the forward model and the accuracy with which the error estimates can be modeled.

Zou et al. [1995] investigated the potential impact of atmospheric RO refractivity measurements, in the context of a four-dimensional variational data assimilation method, and found that the accuracy of the derived water vapor field was significantly better than that obtained through the analytic retrieval technique. Assimilation of the refractivity measurements also provided useful temperature information. *Kuo et al.* [1998] concluded that RO refractivity measurements are likely to have a significant impact on short-range operational NWP, with the caveat that the number of GPS receivers will have to be increased before the full potential impact of this measurement could be realized. *Poli et al.* [2000] performed some preliminary analysis of the GPS/MET observations using the optimal estimation inverse method (also known as one-dimensional variational assimilation) described by *Healy and Eyre* [2000], which assimilates refractivity observations. *Poli et al.* [2000] use the NASA Data Assimilation Office GEOS model to form the a priori. By comparing retrieved profiles with collocated radiosonde profiles, they show that GPS measurements significantly improve the analyses of temperature in the troposphere and lower stratosphere compared to the a priori used.

Palmer et al. [2000] describe the optimal estimation inverse method used to invert the GPS/MET bending angle observation, discussed quality control issues that arise using this method and investigate results from an ensemble of simulated retrievals. *Palmer et al.* [2000] show that GPS RO bending angle observations have the potential to improve NWP analyses of temperature and water vapor between the upper stratosphere and throughout the troposphere. Surface pressure is also retrieved using this method. *Palmer et al.* [2000] found that retrieved surface pressure values are more accurate when bending angle measurements reached near-surface altitudes. The work presented here is the second part of the overall evaluation of the optimal estimation inverse method outlined by *Palmer et al.* [2000], in which we apply this method to real GPS/MET bending angle observations and compare retrieved profiles of temperature, humidity, and surface pressure to correlative data.

A brief description of the optimal estimation inverse method used is presented in section 2. The GPS/MET data set used is described in section 3. Details of the retrievals using the optimal estimation inverse method and the GPS/MET data set are discussed in section 4, and the correlative data used to evaluate these retrievals is described in section 5. Results from the intercomparison are shown and discussed in section 6. We conclude the paper with a discussion of the results shown.

2. Description of the Optimal Estimation Inverse Method Used

Here we outline the optimal estimation inverse method described by *Palmer et al.* [2000] (further information can be found in the work of *Rodgers* [2000]). The rationale behind optimal estimation is to minimize a cost functional $\mathbf{J}(\mathbf{x})$ (or to solve $\nabla_{\mathbf{x}}\mathbf{J}(\mathbf{x})=0$), which measures the degree of fit of

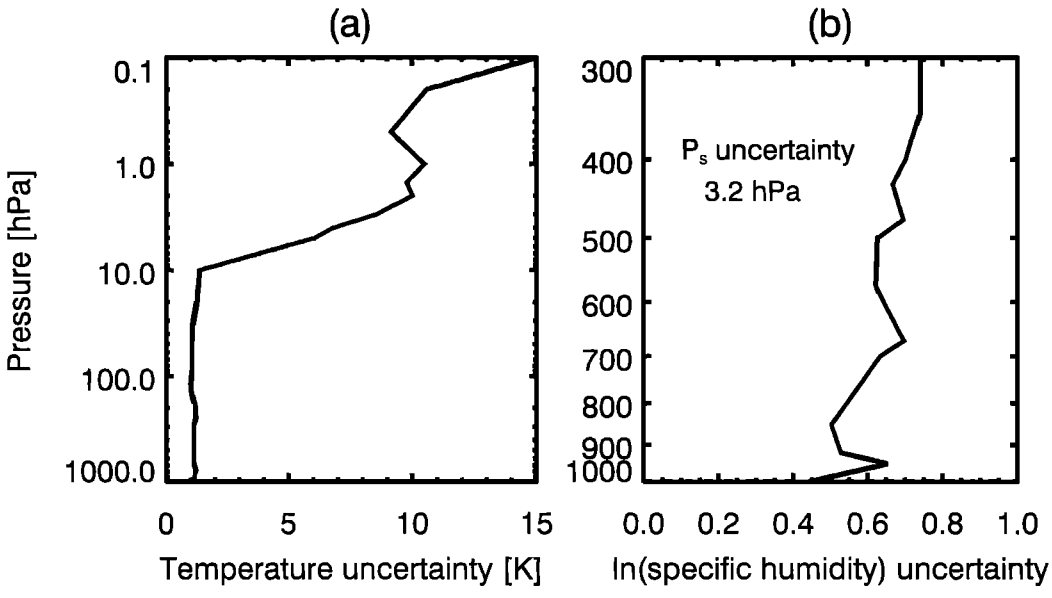

Figure 1. Square root values of the principal diagonal of the ECMWF forecast error covariance matrix. Figures 1a and 1b show the assumed uncertainty for prior temperature and ln(specific humidity), respectively, with the assumed prior uncertainty for the surface pressure element inset of Figure 1b.

estimates of the atmospheric state to the measurements, to some prior information and possibly to some other physical or dynamical constraints. In this case, $\mathbf{J}(\mathbf{x})$ is given by

$$\mathbf{J}(\mathbf{x}) = [\mathbf{y}^o - \mathbf{y}(\mathbf{x})]^T \mathbf{E}^{-1} [\mathbf{y}^o - \mathbf{y}(\mathbf{x})] + (\mathbf{x} - \mathbf{x}^b)^T \mathbf{C}^{-1} (\mathbf{x} - \mathbf{x}^b), \quad (1)$$

where $\mathbf{y}^o$ and $\mathbf{y}(\mathbf{x})$ represent the observation vector and the estimated observation vector, calculated from the state vector using a forward model; $\mathbf{E}$ describes the error characteristics of the observations $\mathbf{y}^o$; $\mathbf{x}^b$ and $\mathbf{x}$ represent the background (also known as the a priori) and updated state vectors, respectively; and $\mathbf{C}$ describes the error characteristics of the a priori state vector.

The observation vector $\mathbf{y}^o$ that comprises GPS/MET bending angle observations is discussed in section 3. The size of $\mathbf{y}^o$ is typically 100–200 elements, spanning a vertical range 0–60 km. The estimated observation vector $\mathbf{y}(\mathbf{x})$ is calculated using the forward model described by *Eyre* [1994].

The measurement error covariance matrix $\mathbf{E}$ comprises the observation noise, errors associated with forward modeling parameters, and forward model error (which includes representativeness error [*Lorenc*, 1986]). The observation errors are taken from *Luntama* [1997] which include thermal noise, residual errors from the ionospheric correction, local multipath, orbit determination accuracy, and clock instabilities of the receiver and the GPS satellites and ground stations. *Syndergaard* [1999] attributes GPS/MET bending angle fluctuations in the upper stratosphere (of the order of 10^{-5} radians) to residual errors from the receiver satellite clock in the calculation of the phase delay of the measured signal. A suitable error is attached to reflect the upper atmosphere measurements.

The a priori state vector contains 40 temperature elements (1000–0.1 hPa), 15 ln(specific humidity) elements (1000–300 hPa), and a surface pressure element. Specific humidity is expressed as the natural logarithm of specific humidity because forecast errors in this quantity are more constant than in specific humidity. The simulation study in the *Palmer et al* [2000] work used NWP analyses from the UK Meteorological Office (UKMO) to form the a priori and first guess. Because of known biases (relative to European Centre for Medium-Range Weather Forecasts (ECMWF) NWP analyses) at the model top for the time period described by the data set used here (summer 1995) (S. Milton, UKMO, personal communication, 1998), we have used ECMWF NWP data to form the a priori profiles, in conjunction with the error statistics of the a priori data. CIRA 1986 climatology is assumed above the ECMWF model, accounting for the latitudinal and seasonal variation of the profiles. This climatology provides reasonable a priori information in the upper stratosphere.

The a priori error covariance matrix $\mathbf{C}$ (Figure 1) is generated from radiosonde-forecast differences between surface–50 hPa, and upper stratosphere values were found by linear regression. This matrix is based on *Eyre* [1989] and attuned to the ECMWF NWP model. The temperature and ln(specific humidity) interquantity covariance values have been set to zero. These interquantity covariances are not well known and assuming zero covariance between them is more conservative than an erroneous covariance. The surface pressure element is uncorrelated with both temperature and ln(specific humidity). It is necessary to consider the errors associated with the CIRA climatology used to form the a priori above the ECMWF analyses. We have retained those values defined by *Palmer et al.* [2000]. In general, if the standard deviation values from the

diagonal elements of the forecast error covariance matrix are smaller than the uncertainties assumed for the climatology, then the climatological errors are used at the levels in the upper atmosphere described by the CIRA climatology (off-diagonal elements remain the same): at latitude θ, for $|\theta| \geq 45°$, σ = 15 K (winter) and 5 K (summer) and for $|\theta| \leq 45°$, σ = 5 K. The uncertainty of the a priori temperature for the ECMWF NWP data is generally less than that of the UKMO a priori temperature used in the simulation study [*Palmer et al.*, 2000], so the GPS/MET retrievals are more tightly constrained to the a priori temperature. There is less a priori constraint to the water vapor and surface pressure.

Palmer et al. [2000] uses the Levenberg-Marquardt (LM) iterative method to minimize $\mathbf{J}(\mathbf{x})$ [*Press et al.*, 1992]:

$$\begin{aligned}\mathbf{x}_{i+1} &= \mathbf{x}^{\mathrm{b}} + [(1+\gamma)\mathbf{C}^{-1} + \mathbf{K}^{\mathrm{T}}\mathbf{E}^{-1}\mathbf{K}]^{-1} \\ &\quad [(\mathbf{K}^{\mathrm{T}}\mathbf{E}^{-1}(\mathbf{y}^{\mathrm{o}} - \mathbf{y}(\mathbf{x}_i))) + \\ &\quad (\gamma\mathbf{C}^{-1} + \mathbf{K}^{\mathrm{T}}\mathbf{E}^{-1}\mathbf{K})(\mathbf{x}_i - \mathbf{x}^{\mathrm{b}})], \qquad (2)\end{aligned}$$

where $\mathbf{K}$ is $\nabla_{\mathbf{x}_i}\mathbf{y}(\mathbf{x}_i)$, γ is a nondimensional weighting factor (for increasing values of γ, this minimization method degenerates into the method of steepest descent), and all other variables are as before. We retain the normal definitions for the a priori and the first guess throughout the paper. The a priori is the best estimate of the state before the measurements are made, which is used here to forward model the observations. The first guess is the starting point for the iterative LM algorithm. For the work shown here, the first guess is the a priori.

3. Description of the GPS/MET Data Set Used

In general, useful data from the GPS/MET receiver are found during "prime times", corresponding to time periods when the military anti-spoofing encryption of the GPS signal is disabled. *Rocken et al.* [1997] report four such periods since the launch of the GPS/MET instrument in April 1995 to February 1997. The purpose of the work shown in this paper is to demonstrate the potential of the bending angle observations, using the optimal estimation inverse method, rather than to validate the observations themselves, so only a relatively small data set (560 occultations) is used for the statistics shown. The 10-day data set used here is from prime-times 1 (May 1995) and 2 (June, July and August 1995) and represents some of the earliest data available [*Kursinski et al.*, 1996]. The selection of the data were largely based upon receiver signal to noise and the relatively large number of occultations that reach near-surface altitudes. Processing of the atmospheric time delay from GPS/MET instrument used here was carried out by the Jet Propulsion Laboratory (JPL) to compute bending angle values as a function of impact parameter and is similar to that methodology described by *Rocken et al.* [1997].

4. Computing Optimal Estimates From GPS/MET Bending Angle Observations

Convergence criteria and quality control procedures outlined by *Palmer et al.* [2000] were used to filter out profiles that either did not converge or converged on to a solution with an unrealistic χ^2 value (a χ^2 value higher than the theoretical value, given the degrees of freedom, at the 99.9% level); 118 retrievals failed this quality control, representing 21% of the total number of occultation profiles in the data set used. All failed profiles were due to the solution converging on to unrealistically high χ^2 values, as opposed to non convergence. These profiles are omitted from subsequent comparisons with correlative data.

To investigate whether a particular geographical region is responsible for these failed retrievals, they are separated into polar, midlatitude, and tropics by virtue of their mean latitude θ (corresponding typically to the midtroposphere). For this purpose the polar regions are defined as $|\theta| \geq 70°$, the tropics region is defined as $|\theta| \leq 30°$; and the midlatitude region is defined between the polar region and the tropics. The percentage of profiles that fail in each defined region shows a large disparity between the polar regions (4%) and the tropics (27%) (compare midlatitude 15%). We find that the majority of the retrievals that fail quality control in the tropics have large χ^2 values that derive from large a priori−observation differences in the lower atmosphere (less than 15 km). A possible reason for these failed retrievals is that modeled and observed water vapor are too different for the a priori and observation error constraints to reconcile. Estimates of bending angle errors introduced by horizontal refractivity structure along the receiver line of sight direction are derived from midlatitude temperature and humidity fields [*Palmer*, 1998] and describe typical errors in that region. This error dominates the error budget described by $\mathbf{C}$ in the lower atmosphere, even for midlatitudes [*Palmer et al.*, 2000]. Aside from extreme case scenarios these global errors are found to be sufficient for the purpose of demonstrating the inverse method [*Palmer et al.*, 2000]. The χ^2-based quality control has proven to be invaluable for the one-dimensional inverse problem by indentifying and removing spurious retrievals.

5. Description and Preparation of Correlative Data

To validate optimal estimation retrievals, several different sources of correlative data are used. Although the optimal estimate has been computed for 1000−0.1 hPa [*Palmer et al.*, 2000] (reflecting the vertical range of occultation data), statistics are shown for 1000−10 hPa which reflect the vertical range described by analyses and radiosondes. Bending angle observations have relatively little impact on optimal retrievals above 10 hPa [*Palmer et al.*, 2000], because of the large stratospheric observation noise value assumed [*Syndergaard*, 1999].

5.1. Radiosondes

Radiosonde data have been used to validate the GPS/MET radio occultation observations because they typically possess high vertical resolution, resolving features with vertical scales of a few tens of meters. However, the distribution of radiosondes is sparse (particularly in the Southern Hemisphere) and their temporal coverage is not continuous,

with typically only two launches per day (nominally at 0000 and 1200 UT). The global corrected radiosonde data set used here is originally from the National Centers for Environmental Prediction (NCEP).

The nearest radiosonde to each collocation is found first by considering the nearest launch time. Second, the nearest radiosonde in space is found using the mean latitude and longitude of the occultation and the geographic position of each radiosonde and computing the great circle distance. Only radiosondes that are within ±3 hours and a distance of 300 km from the observations are used in this study. Using this method, a total of 50 radiosondes are "close enough" for this comparison study.

5.2. NWP Analyses

Because closely correlative radiosonde profiles are rare, NWP analyses are also used to validate the retrievals. It is noted that NWP models use atmospheric observations, for example, radiosondes, to initialize model fields, therefore any NWP model output should not disagree too much with reasonably collocated radiosondes. Although the majority of NWP centers generally use the same set of global observations, their different analysis methods and dynamical representations should mean that analyses from different NWP models are largely independent. This point is particularly important since model analyses are used for the retrieval a priori (and first guess).

The UKMO NWP data from short-range forecasts provided by the UKMO unified model [*Cullen*, 1993]. The model from which the data are derived has 19 levels, which are expressed on hybrid-sigma pressure coordinates (surface−10 hPa). The model version has a resolution of 0.833° (180°/217) latitude and 1.25° (360°/288) longitude. Model fields are interpolated in time and in space to occultation event positions, using the mean latitude and longitude of each occultation.

5.3. Analytic Inverse Method Retrievals

The analytic inverse method represents the conventional method of retrieving profiles of refractivity from radio occultation observations [*Fjeldbo and Eshleman*, 1968] and, subsequently, profiles of temperature or specific humidity. This is a useful source of comparative data since results from this method have already been compared against independent sources of atmospheric information [*Rocken et al.*, 1997]. Retrievals from the analytic inverse method are not strictly independent from the optimal estimation retrieval since they use the same bending angle observations. However, the two inverse methods should be sufficiently different that a comparison provides useful information.

A relatively simple approach has been adopted for the analytic inverse method, in which ECMWF analyses are used to initialize the hydrostatic relation at the NWP model top [c.f. *Steiner et al.*, 1999]. The ancillary data used to account for the presence of water vapor on the refracted signal in the lower atmosphere are collocated UKMO analyses. Values of ln(specific humidity) (from partial water vapor pressure) are also retrieved using this method but are restricted to the tropics so reasonably large values of water vapor are guaranteed.

6. Intercomparison Results

The statistical comparison shown in this section is based on the 10-day data set described in section 3. The impact of the observations on reasonable a priori estimates is examined by computing the mean bias (retrieval minus a priori) and its standard deviation. The optimal estimates are then compared with several sources of correlative data by looking at the ensemble mean bias values and their standard deviations. Two occultation events are examined in detail with correlative data to gain further insight into the potential of the observations using the retrieval method. The mean of a vector x and its standard deviation σ_x is given by

$$\overline{x} = \frac{1}{N}\sum_{i=1}^{N} x_i, \tag{3}$$

$$\sigma_x = \sqrt{\frac{1}{N-1}\sum_{i=1}^{N}(x_i - \overline{x})^2}. \tag{4}$$

These definitions will be retained throughout the paper.

6.1. Impact on a Priori Estimates

The mean bias and its standard deviation of (retrieval minus a priori) are computed so that the extent to which the optimal estimation retrieval deviates from the a priori used can be estimated. *Palmer et al.* [2000] showed that the surface pressure retrieval accuracy was related to whether the bending angle observations reached the surface and that only surface pressure retrievals that correspond to bending angle profiles terminating in the lower atmosphere should be considered. Only occultations that extend to altitudes less than 700 hPa will be considered, resulting in 26% of the occultations being retained.

Figure 2 shows that the mean temperature differences between the retrieval and its a priori are largest generally at heights typical of the tropopause, consistent with the observations resolving the tropopause more accurately than the NWP model and toward the top of the ECMWF model. Mean ln(specific humidity) differences show little structure; typically, retrievals have less (more) water vapor below (above) 700 hPa. Table 1 shows the surface pressure retrieval−a priori statistics. The global mean bias is -2.2 ± 5.7 hPa. These values represent large deviations from analyses. These differences are examined further by separating the occultations into polar, midlatitude, and tropics geographic regions using the definitions defined in section 4. Statistics from midlatitude retrievals are not shown because they exhibit similar structure and magnitude to the overall statistics.

Polar temperature retrievals show a cold bias (0.5 K) in the lower troposphere and a warm bias (1 K) in the upper troposphere/stratosphere. Polar ln(specific humidity) retrievals show there is more (15%) water vapor in the retrievals at altitudes above 700 hPa and less below (10%). Cold, dry conditions in polar atmospheres allow the radio

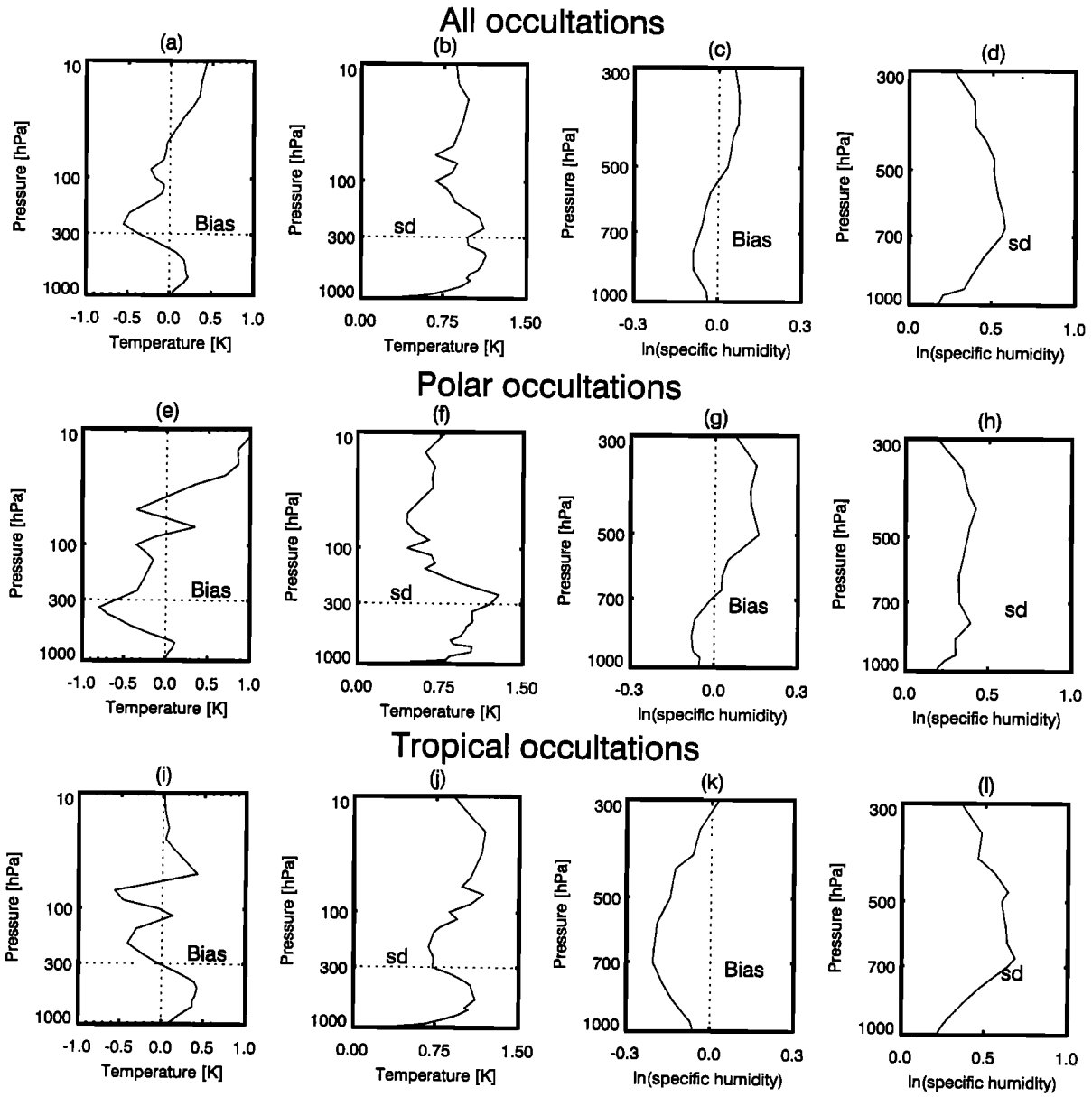

Figure 2. Optimal retrieval – a priori statistics. Figures 2(a)–2(l) are sectioned into three lines, each with four plots. The first (third) and second (fourth) plots on each line correspond to the mean difference and its standard deviation between the retrieved and a priori temperature (ln(specific humidity)). The dashed horizontal line denotes 300 hPa. A positive bias is where the a priori is smaller.

occultation technique to penetrate close to the ground, thus containing a relatively large amount of surface pressure information [*Palmer et al.*, 2000]. Retrieved surface pressure values have a large negative mean bias of 4.9±2.9 hPa.

Retrieved temperature profiles in the tropics have a warm (cold) bias at altitudes below (above) 300 hPa. The 300 hPa altitude level represents the height at which the optimal inverse method starts to retrieve temperature and humidity simultaneously. The ln(specific humidity) retrieval shows a large negative bias which increases as a function of depth. Reduction of the retrieval bias at the lowest altitudes is a direct consequence of the relatively small number of occultations reaching heights sufficiently near the surface. Few occultations reached pressures greater than 700 hPa, and retrieved surface pressure values have a large positive bias (>4 hPa). These features are consistent with those described by *Kursinski et al.* [2000] which they attribute to the lack of water modeled above 300 hPa. To compensate for the "missing" water vapor, the solution must increase the dry density above 300 hPa by increasing the pressure at these heights and decreasing the temperature between 200 hPa and 300 hPa (~12 km). To increase the hydrostatic pressure at a particular height, the solution increases the temperature below 300 hPa (<0.5 K) and increases surface pressure by ~3.8 hPa.

We investigated several retrievals in the tropics using the matrix of contribution functions $\mathbf{D}$ [*Rodgers*, 1976], which describes how each measurement in the observation vector

$\mathbf{y}^o$ contributes to the retrieved atmosphere state $\hat{\mathbf{x}}$, i.e., $\partial\hat{\mathbf{x}}/\partial\mathbf{y}^o$. Retrievals involving bending angle profiles, which span into the lower atmosphere, generally have contribution functions that peak at levels corresponding to the measurement height at which they are measured, and the surface pressure contribution function strongly peaks at near-surface altitudes. For the tropical occultations examined, the surface pressure contribution function has a strong peak at 300 hPa, which decreases rapidly above and below this level. This result suggests that the surface pressure increment is associated with bending angle differences above 300 hPa. This result is consistent with the "missing" water vapor argument by *Kursinski et al.* [2000]. The large surface pressure and temperature compensation effect makes results at higher altitudes in the tropics difficult to interpret.

6.2. Comparison with Correlative Data

Figure 3 shows the statistics for all the occultations compared with all sources of correlative data. The impact of the observations on the a priori is not obvious if the occultation data are studied together. It is evident that there is a bias in the UKMO NWP model (triangles) at heights above 100 hPa. Further insight into the statistics is possible if occultations are separated into tropical and polar latitudes using the definitions in section 4.

Polar optimal estimation retrievals agree well with the analytic retrievals (Figure 4) except at altitudes above 50 hPa, owing to ECMWF analyses being used to form the first guess for the analytic inversion. Large differences between the a priori and the analytic retrieval at 100 and 400 hPa are less pronounced in the comparison between the optimal estimation retrieval and the analytic retrieval. This is consistent with Figure 2 where the largest differences between the retrieval and a priori are at heights typical of the tropopause. Comparison with radiosonde data shows better agreement with the a priori than the optimal estimation retrieval, which is consistent with results shown by *Rocken et al.* [1997]. This is probably due to the radiosonde profiles being used to help initialize the NWP model. Water vapor differences between the different sources of data are slight.

Optimal estimation retrievals in the tropics are shown in Figure 5. The positive (negative) bias above (below) 400 hPa shown between optimal estimation inverse method and the analytic retrievals is less than that shown between the a priori and analytic retrieval. In this region, there is improved agreement between optimal estimation retrieval and radiosonde data, relative to the a priori comparison with the radiosonde data, with a smaller bias and a reduced standard deviation. This is contrary to the water vapor comparison. The UKMO analyses are higher than both the ECMWF analyses and the optimal estimation retrievals using GPS/MET bending angle observations. Application of the GPS/MET observations using the optimal estimation inverse method has the effect of decreasing the amount of water vapor further. Reduction in the bias in the lower height levels reflects the small number of observations that are present below 700 hPa.

Table 2 shows the surface pressure comparison between retrievals for which GPS/MET observations reach altitudes of less than 700 hPa, and UKMO and ECMWF analyses. Differences between the two analyses are less than 0.8 hPa (the ECMWF has a negative bias) and the standard deviation values are typically less than 4 hPa. In contrast, the difference between the retrieval and the UKMO analyses is typically greater than 4 hPa with standard deviation values 5 hPa, which is similar to the differences between the a priori (ECMWF analyses) and the retrieval. Tropical occultations have a positive bias relative to analyses. Surface pressure retrievals in the tropics have already been shown to be associated with a compensation effect due to omission of water vapor above 300 hPa so it is unsurprising that a comparison with analyses shows a large difference.

6.3. Individual Occultations

Here we show two occultations that exemplify the optimal estimation inverse method, one at high latitude and one at low latitude. Figure 6 shows a typical high latitude occultation (also shown by *Kursinski et al.* [1996]). Cold, dry conditions allow temperatures from the analytic inverse method to be derived accurately to within 0.5 km of the surface [*Kursinski et al.*, 1996]. The collocated radiosonde agrees well with the analytic inversion with differences of less than 1 K for most of the troposphere. The optimal estimation appears to "shadow" the analytic inversion, resolving small-scale features not seen by the analyses. Figures 6c and

Table 1. Mean Bias and Standard Deviation Statistics of the Difference Between the Surface Pressure Retrievals for Occultations that Reach Altitudes of $\leq$ 700 hPa and a Priori. Data shown have been filtered to remove retrievals that do not pass a χ^2 quality control test (see text for details).

Occultation that Reach $P \geq 700$ hPa	Retrieval − a Priori [hPa]		Number of Profiles
	Bias	σ	
Global	-2.22	5.72	118
Polar regions	-4.91	2.89	17
Tropics	3 84	4.88	9

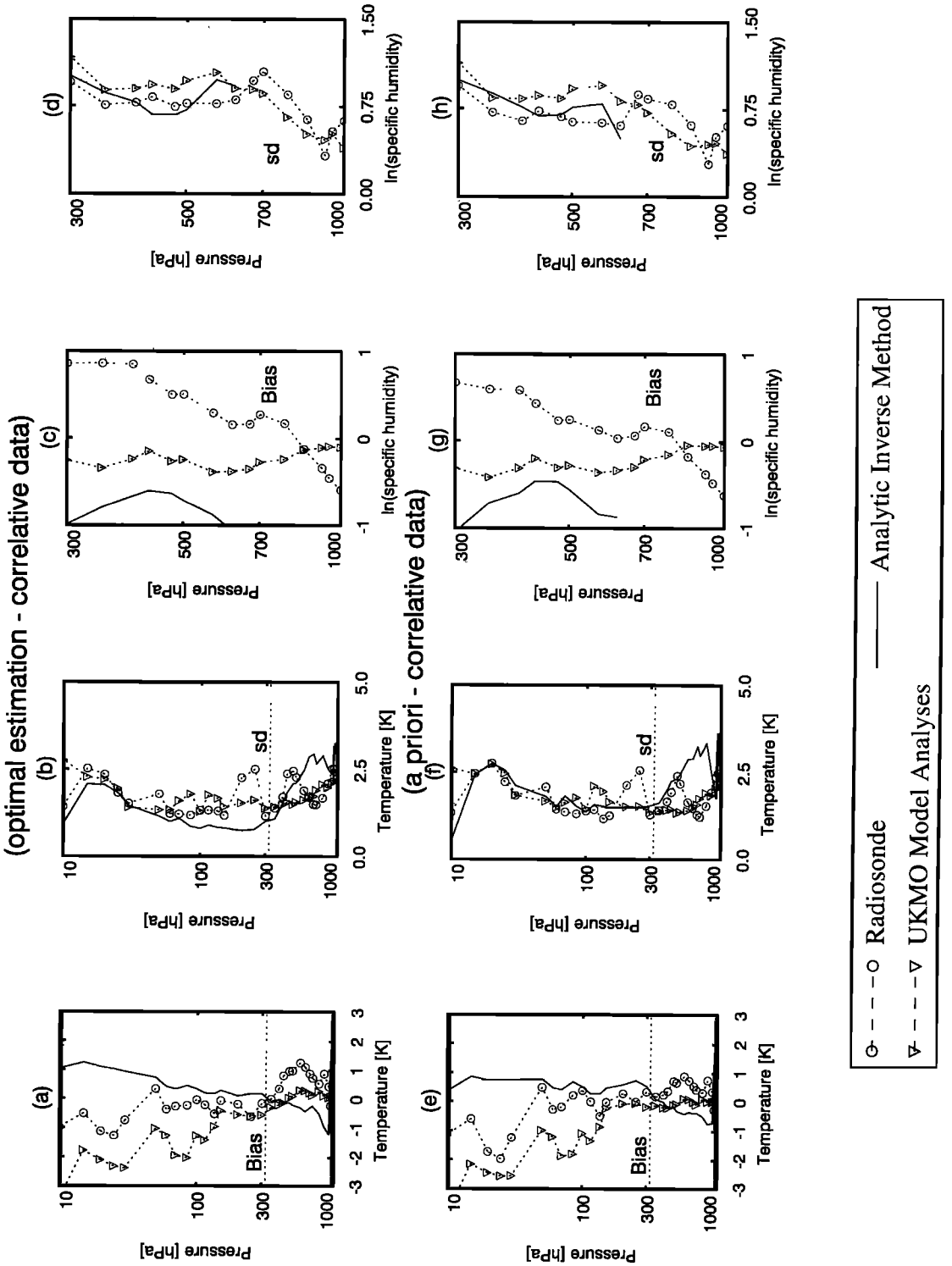

Figure 3. Mean bias and standard deviation global statistics between the retrieval/a priori and correlative UKMO analyses, radiosondes, and results from the analytic inversion. (a–d) Retrieval–correlative data comparison for temperature and ln(specific humidity), and (e–h) the a priori–correlative data comparison. The dashed horizontal line denotes 300 hPa. A positive bias is where the correlative data are smaller.

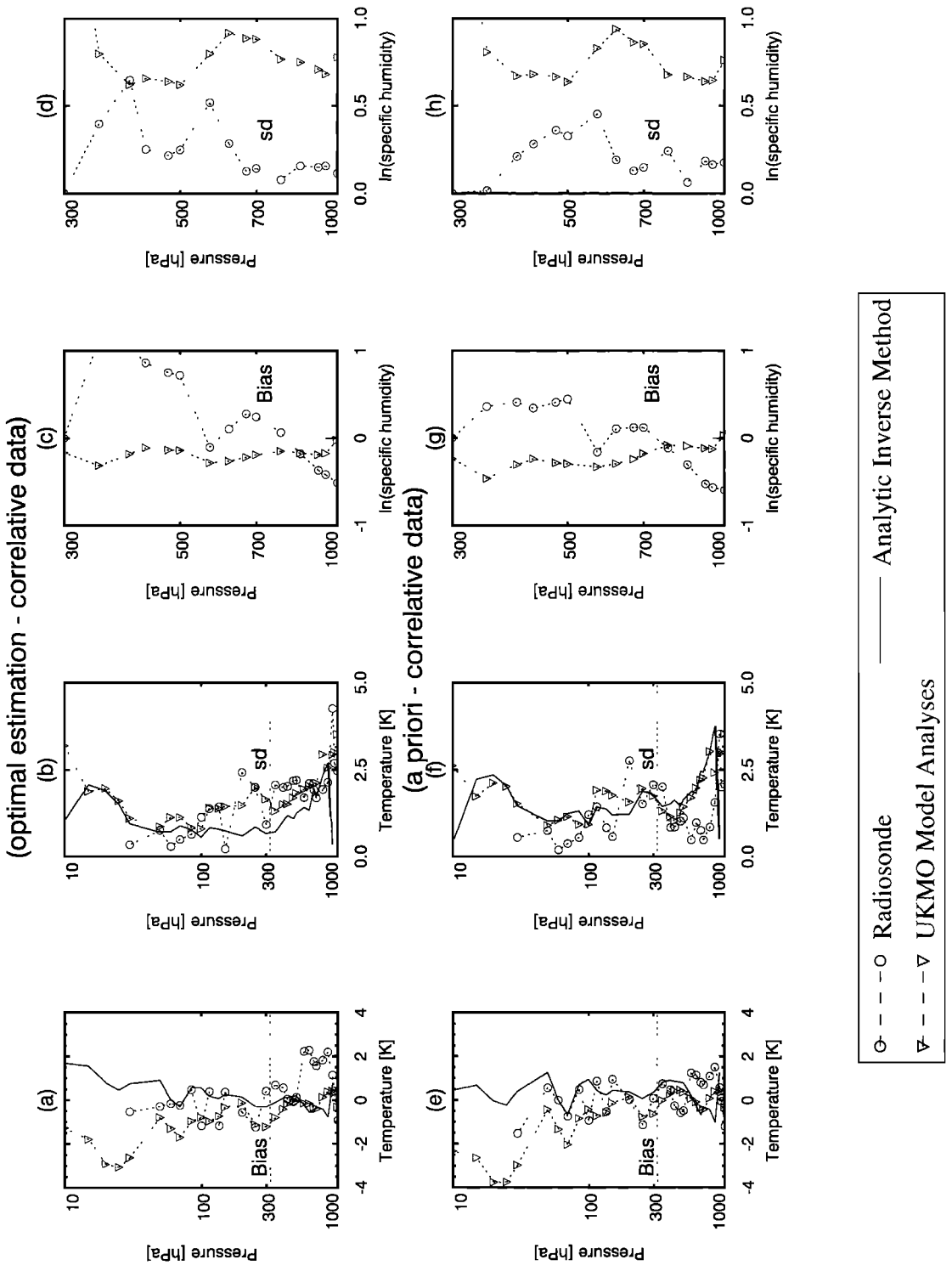

Figure 4. As Figure 3 but for polar profiles only.

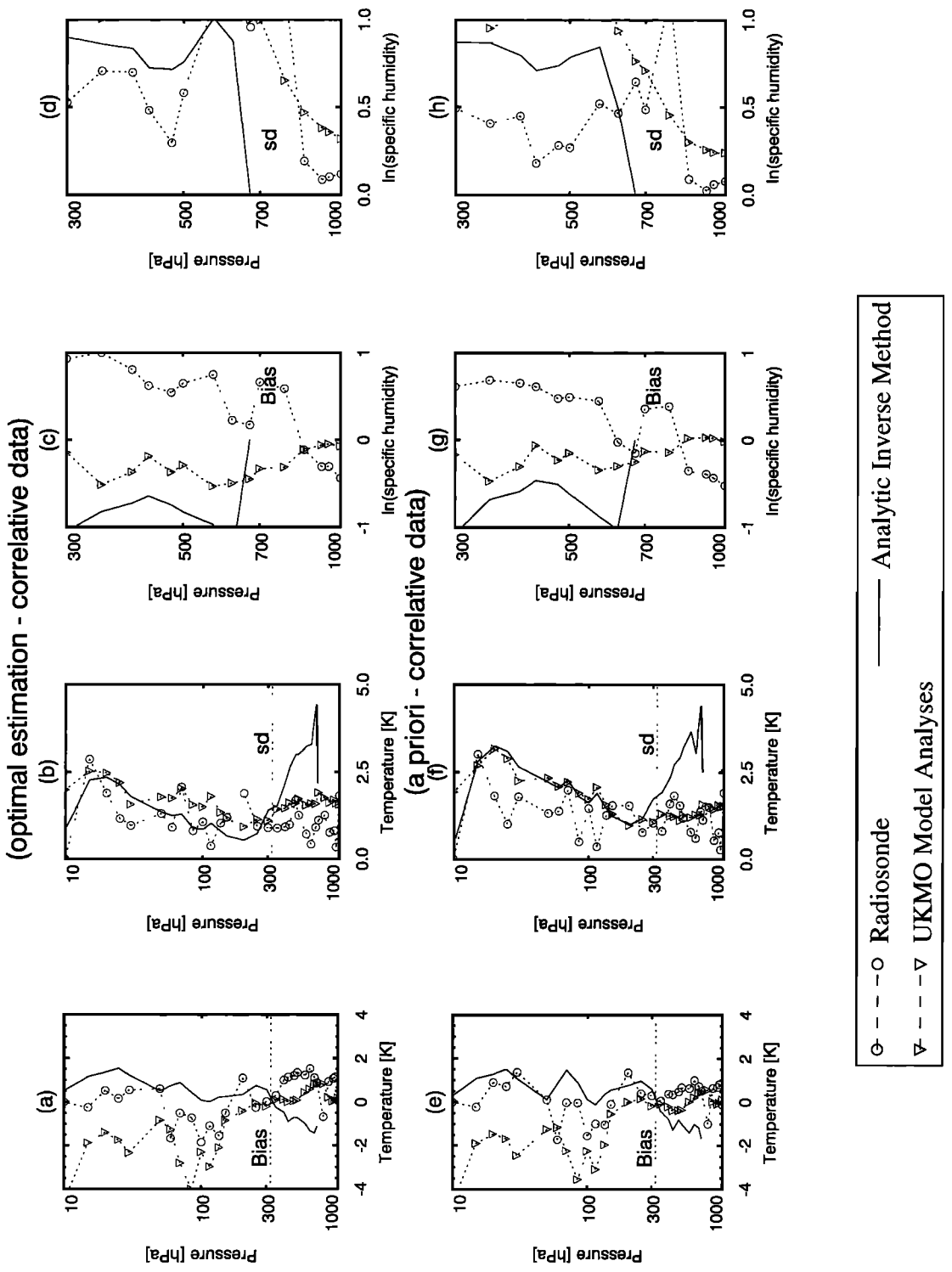

Figure 5. As Figure 3 but for tropical profiles only.

Table 2. Mean Bias and Standard Deviation Statistics of the Difference Between the Surface Pressure Retrieval and UKMO Analyses, and Between a Priori (ECMWF Analyses) and the UKMO Analyses. Values within parantheses represent statistics of the difference between the a priori and the UKMO analyses. The data represent results from considering occultations whose lowest pressure is larger or equal to 700 hPa.

Occultation that Reach $P \geq 700$ hPa	Retrieval − UKMO [hPa] (a Priori − UKMO)		Number of Profiles
	Bias	σ	
Global	-3.00 (-0.78)	6.81 (3.60)	118
Polar regions	-5.75 (-0.81)	4.29 (4.38)	17
Tropics	4.01 (-0.17)	5.65 (1.13)	9

6d show a marked decrease in the specific humidity optimal estimate (converted from ln(specific humidity) to represent a physical quantity) relative to the ECMWF analyses and radiosonde. The relatively large percentage difference shown in Figure 6d above 500 hPa reflects the large variation between relatively small amounts of water vapor associated with this occultation. The magnitude of these variations is comparable with the difference between models in the polar regions (Figure 4). Figure 6c also shows that the surface pressure retrieval decreases relative to the ECMWF (used to form the a priori) and UKMO model analyses value (989.23 hPa).

Figure 7 shows a typical low-latitude occultation. For this particular occultation, reasonable observations terminate at approximately 500 hPa. At altitudes about the tropopause the temperature optimal estimate agrees well with the analytic inverse method, again resolving the tropopause not shown by the analyses (~2 K difference). Immediately above the tropopause the analytic retrieval develops a cold bias (relative to the optimal estimate) and follows the structure of the collocated radiosonde. The cold bias developed is of the order of 6 K, which is considerably larger than the prescribed a priori constraint, so it is unsurprising that this structure is not resolved by the optimal estimate. Farther into the troposphere, the analytic temperature retrieval develops an increasing warm bias relative to the optimal estimate and analyses. This bias is due to the inadequacy of the low-water correction for the analytic temperature retrieval in the presence of large water vapor concentrations. At low altitudes the optimal estimate agrees with analyses with differences of less than 1 K as a consequence of no observations near the surface. The specific humidity comparison is shown in Figure 7c. The specific humidity optimal estimate shows good agreement with the analytic retrieval with differences of <10%. The radiosonde has a warm bias relative to both the analyses and the retrievals. A possible reason for this is the relatively large spatial collocation distance from the occultation event. The surface pressure retrieval is larger than both the a priori and the UKMO analyses (1010.97 hPa). Since reasonable bending angle observations for this occultation terminate at 500 hPa, the retrieved value is of limited value.

7. Discussion

Bending angle observations of Earth's neutral atmosphere from the radio occultation technique are largely affected by and therefore contain information about temperature and humidity in the stratosphere and troposphere. In the troposphere, where water vapor can contribute significantly to the observation, it is impossible to separate temperature and humidity effects by using the GPS RO observations alone. The conventional method of inverting bending angle measurements involves an integral transform to obtain a profile of refractivity (as a function of geometric height) [*Fjeldbo and Eshleman*, 1968]. The hydrostatic relation is used to obtain pressure and temperature from refractivity via density. To separate the effect of temperature and humidity, a correction can be made in this retrieval step, involving use of a priori specific humidity profile information. When the water vapor signal becomes significant, partial water vapor pressure is retrieved assuming a priori temperature profile information. This represents a suboptimal method of retrieving temperature and humidity since there is no guarantee of consistency between the retrieved temperature and the humidity profiles. An optimal estimation inverse method is able to retrieve temperature and humidity simultaneously from bending angle observations, using a priori data. Retrieving these quantities simultaneously ensures their consistency, unlike the values retrieved using the conventional inverse method. Inhomogeneities along the transmitter–receiver path can introduce bending angle errors. Within the optimal estimation inverse method framework, it is possible to account for these errors, unlike the conventional inverse method. These represent two key advantages of using the optimal estimation inverse method.

We have applied the nonlinear optimal estimation method described by *Palmer et al.* [2000] to GPS/MET bending angle observations. We find that GPS/MET bending angles observations improve upon reasonable NWP analyses for

the troposphere and for much of the stratosphere (global retrieval−a priori differences for temperature, humidity, and surface pressure differences are ~0.5 K, ~10%, and 2 hPa, respectively). Retrieval increments to a priori temperature and humidity information are consistent with the correlative data used. Values of retrieved surface pressure are generally less than analyses, apart from the tropics where the retrievals have a positive bias. Surface pressure increments in the tropics are found to be consistent with a compensation effect for not modeling water vapor above 300 hPa in the inverse method, as suggested by *Kursinski et al.* [2000]

Further insight into the retrievals has been possible by analyzing two individual occultation profiles, one at high and low latitude. The optimal estimation retrievals resolve tropopause structure. Previous evaluation of the data using the analytic inverse method has also noted the ability of GPS/MET observations to resolve such structure [*Kursinski et al.*, 1996]. What is striking about the results shown here is that the characteristic sharp features of the extratropical tropopause are resolved on a relatively small number of model levels, typical of a NWP model, as opposed to retrieving temperature and humidity on a number of levels typical of an occultation (>100). Analysis of the surface pressure retrieval is limited due to the lack of correlative surface pressure data and because much of the data set used does not penetrate heights lower than 1 km. The retrieval

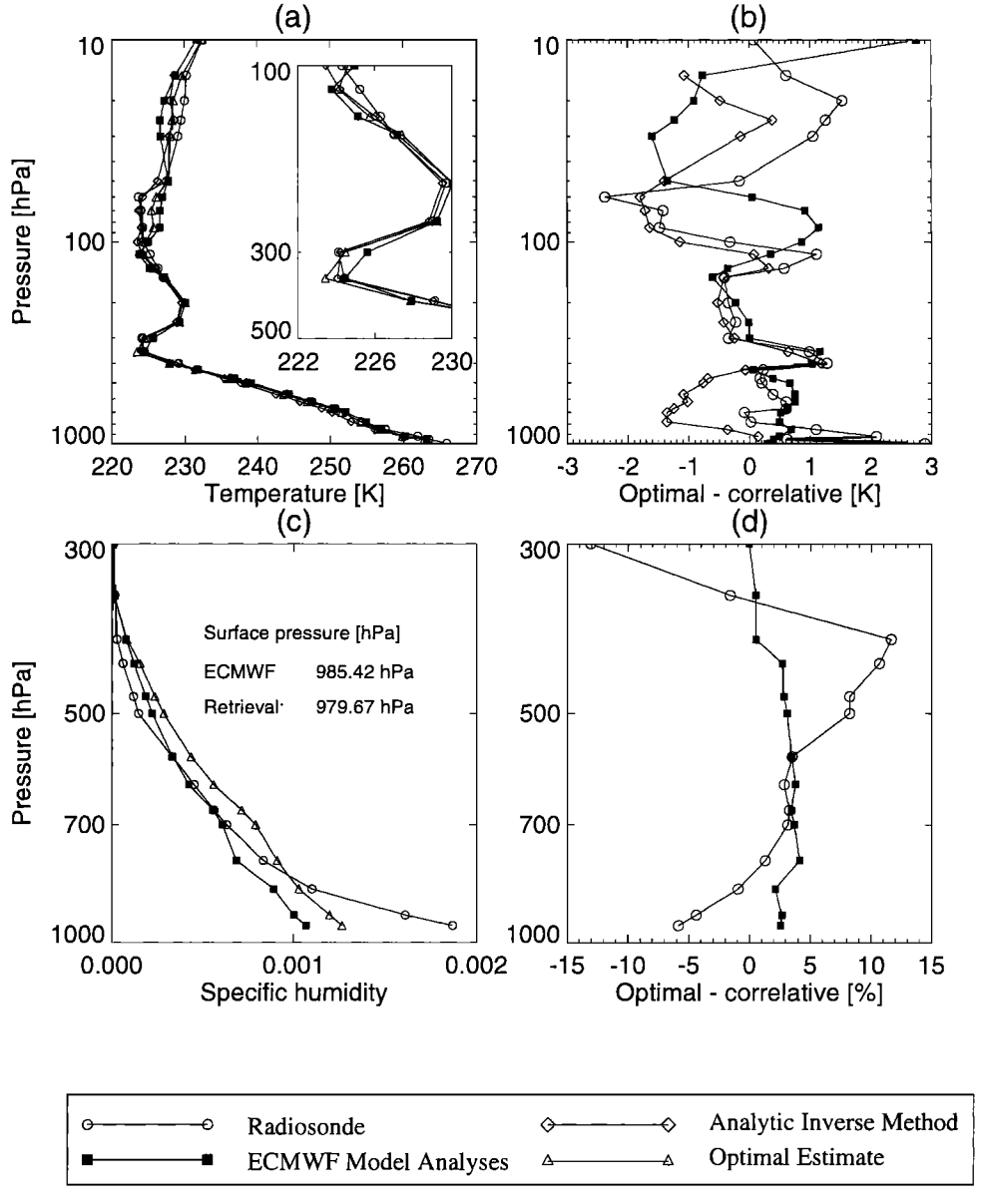

Figure 6. Comparison between a high-latitude occultation (0133 UT, May 5, 1995) and correlative data. The occultation event is obtained at 69.1°N, 277.7°E; the radiosonde is from 68.8°N, 278.8°E at 0000 UT; and model analyses are from 0000 UT. (a) Temperature comparison, (b) temperature differences between the optimal estimate and the correlative data, (c) specific humidity comparison (with surface pressure comparison inset), and (d) specific humidity differences. The inset in Figure 6a is an enlarged section of the temperature profile shown, corresponding to the tropopause region.

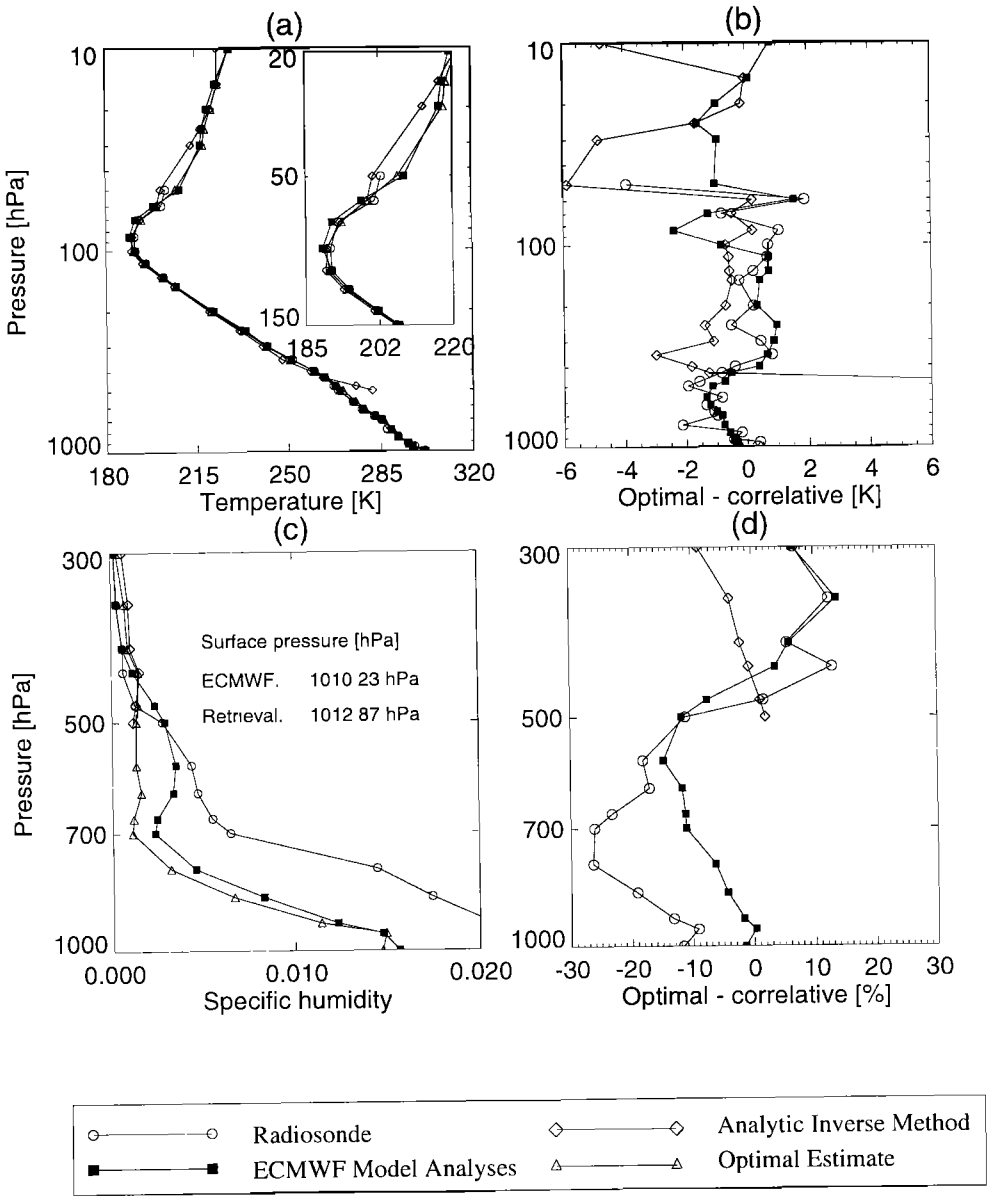

Figure 7. Comparison between a low-latitude occultation (12:40 UT, May 4, 1995) and correlative data, including results from the analytic inverse method. The occultation event is obtained at 7.9°S, 167.5°E; the radiosonde is from 6.0°S, 170.4°E at 1200 UT; and the analyses are taken from 1200 UT. Panels and plotting symbols are as Figure 6.

difficulty in the lower troposphere is believed to be due to sharp vertical gradients in atmospheric refractivity, because of sudden changes in water vapor [*Rocken et al.*, 1997]. Future missions will employ instrumentation which will improve the signal tracking and the signal-to-noise ratio [*Rocken et al.*, 1997].

It should be realized that relatively simple a priori and measurement error covariances have been assumed in this work and represent preliminary estimates. Future work should include improved modeling of these estimates so that they represent temporal and spatial variability. However, results using the preliminary error estimates are encouraging.

Acknowledgments. The authors wish to thank R. Kursinski (JPL, now at the University of Arizona) and S. Leroy (JPL) for many useful comments on earlier work and for providing the GPS/MET data set used here. We gratefully acknowledge the University Corporation for Atmospheric Research for operating the GPS/MET program. We would also like to thank S. B. Healy for constructive criticism on earlier versions of this manuscript, J. P. Luntama for providing the measurement error estimates for the optimal estimation retrievals, and M Gorbunov, R. Wells, and T. Clemons for obtaining the correlative data used.

References

Ahmad, B., and G. L. Tyler, Systematic errors in atmospheric profiles obtained from Abelian inversion of radio occultation data: Effects of large-scale horizontal gradients, *J. Geophys. Res.*, *104*, 3971–3992, 1999.

Cullen, M. P., The unified forecast/climate model, *Meteorol. mag.*, *112*, 1449–1451, 1993.

Eyre, J. R., Inversion of cloudy satellite sounding radiances by nonlinear optimal estimation. I: Theory and simulation for TOVS, *Q. J. R. Meteorol. Soc.*, *115*(489), 1001–1026, 1989.

Eyre, J. R., Assimilation of radio occultation measurements into a numerical prediction system, Eur. Cent. for Medium-Range Weather Forecasts, Reading, England, Tech. Rep. 199, 1994.

Fjeldbo, G., and V. Eshleman, The atmosphere of Mars analysed by integral inversion of the Mariner IV occultation data, *Planet Space Sci.*, *16*, 1035–1059, 1968.

Healy, S. B., and J. R. Eyre, Retrieving temperature, water vapour and surface pressure information from refractive index profiles derived by radio occultation: A simulation study, *Q. J. R. Meteorol. Soc.*, *126*, 1661–1684, 2000.

Kuo, Y.-H., et al., A GPS/MET sounding through an intense upper-level front, *Bull. Am. Meteorol. Soc.*, *79*(4), 617–626, 1998.

Kursinski, E., et al., Initial results of radio occultation observations of Earth's atmosphere using GPS, *Science*, *271*, 1107–1110, 1996.

Kursinski, E. R., G. A. Hajj, K. R. Hardy, J. T. Schofield, and R. Linfield, Observing the Earth's atmosphere with radio occultation measurements using GPS, *J. Geophys. Res.*, *102*, 23,429–23,465, 1997.

Kursinski, E. R., S. B. Healy, and L. R. Romans, Initial results of combining GPS occultations with ECMWF global analyses within a 1DVAR framework, *Earth Planets Space*, *52*, 885–892, 2000.

Lorenc, A., Analysis methods for numerical weather prediction, *Q. J. R. Meteorol. Soc.*, *112*, 1177–1194, 1986.

Luntama, J.-P., Atmospheric profiling with radio occultation, Master's thesis, Dept. of Elect. and Commun. Eng., Helsinki Univ. of Technol., Helsinki, Finland, 1997.

Palmer, P. I., Analysis of atmospheric temperature and humidity from radio occultation measurements, D.Phil. thesis, Oxford Univ., Oxford, England, 1998.

Palmer, P. I., J. J. Barnett, J. R. Eyre, and S. B. Healy, A nonlinear optimal estimation inverse method for radio occultation measurements of temperature, humidity, and surface pressure, *J. Geophys. Res.*, *105*, 17,513–17,526, 2000.

Poli, P., J. Joiner, R. Kursinski, and M. Kolodner, 1dvar analysis of temperature and humidity using GPS radio occultation, in *Proceeedings of the 10th Conference on Satellite Meteorology and Oceanography*, Am. Meterol. Soc., Boston, Mass., 2000.

Press, W. H., B. P. Flannery, S. A. Teuklsky, and W. T. Vetterling, *Numerical Recipes: The Art of Scientific Computing*, Cambridge Univ. Press, New York, 1992.

Rocken, C., et al., Analysis and validation of GPS/MET data in the neutral atmosphere, *J. Geophys. Res.*, *102*, 29,849–29,866, 1997.

Rodgers, C. D., Retrieval of atmospheric temperature and composition from remote measurements of thermal radiation, *Rev. Geophys.*, *14*, 609–624, 1976.

Rodgers, C. D., *Inverse Methods for Atmospheric Sounding: Theory and Practice*, World Sci., River Edge, N.J, 2000.

Steiner, A. K., G. Kirchengast, and H. P. Ladreiter, Inversion error analysis and validation of GPS/MET occultation data, *Ann. Geophys.*, *17*, 122–138, 1999.

Syndergaard, S., Retrieval analysis and methodologies in atmospheric limb sounding using the gnss radio occultation technique, Ph.D. thesis, Danish Meteorol. Instit., Copenhagen, Denmark, 1999.

Ware, R., et al., GPS sounding of the atmosphere from low-Earth orbit: Preliminary results, *Bull. Am. Meteorol. Soc.*, *77*, 19–40, 1996.

Zou, X., Y. H. Kuo, and Y. R. Guo, Assimilation of atmospheric radio refractivity using a nonhydrostatic adjoint model, *Mon. Weather Rev.*, *123*, 2229–2249, 1995.

J. J. Barnett, Department of Physics, Clarendon Laboratory, Oxford, OX1 3PU, England, U.K., (j.barnett1@physics.ox.ac.uk)

P. I. Palmer, Division of Engineering and Applied Science, and Department of Earth and Planetary Sciences, Harvard University, Cambridge, MA 01238 (pip@io.harvard.edu)

(Received July 31, 2000; revised March 26, 2001;
accepted March 30, 2001.)